



Repositorio Institucional de la Universidad Autónoma de Madrid

<https://repositorio.uam.es>

Esta es la **versión de autor** del artículo publicado en:

This is an **author produced version** of a paper published in:

Advanced Materials Technologies 2 (8): 1700024

DOI: <http://dx.doi.org/10.1002/admt.201700024>

Copyright: © 2017 Willey

El acceso a la versión del editor puede requerir la suscripción del recurso

Access to the published version may require subscription

DOI: 10.1002/ (Admt.201700024)

Article type: Full Paper

Plasmonic Enhancement in the Fluorescence of Organic and Biological Molecules by Photovoltaic Tweezing Assembly

Iris Elvira¹, Juan F. Muñoz-Martínez^{1,2}, Mariano Jubera³, Angel García-Cabañes¹, José L. Bella⁴, Patricia Haro-González¹, María A. Díaz-García⁵, Fernando Agulló-López¹ and Mercedes Carrascosa^{1}*

*Corresponding Author: E-mail: m.carrascosa@uam.es

¹Departamento de Física de Materiales, Universidad Autónoma de Madrid, 28049 Madrid, Spain

²Departamento de Mecánica de Fluidos y Propulsión Aeroespacial, Universidad Politécnica de Madrid, 28040 Madrid, Spain

³Scientific Division, Centro de Láseres Pulsados (CLPU), 37185 Villamayor (Salamanca), Spain

⁴Departamento de Biología, Universidad Autónoma de Madrid, 28049 Madrid, Spain

⁵Departamento de Física Aplicada and Instituto Universitario de Materiales, Universidad de Alicante, 03080 Alicante, Spain

Keywords: (optoelectronic tweezers, nanoparticle optical manipulation, plasmonic luminescence enhancement, enhanced biomolecule fluorescence, bulk-photovoltaic effect)

The potential of photovoltaic tweezers to produce plasmonic platforms for fluorescence enhancement of organic or biological molecules is demonstrated. 1D and 2D patterns of silver nanoparticles have been produced on the surface of LiNbO₃:Fe substrates using this photovoltaic tool, which allows depositing in parallel a large number of particles in

accordance with imposed 1D and 2D light profiles. The nanoparticle patterns reveal a variety of plasmonic features whose resonances cover a broad spectral range and are able to produce efficient fluorescence enhancement. First a remarkable average enhancement factor of ten has been measured for Disperse Red 1 organic molecules deposited on the patterns. Clear enhancements have been also obtained from fluorescein labeled biological molecules (DNA and asynthetic peptide). Finally, the possibility of using the photo-electrically generated metallic patterns with other substrates is also demonstrated by enhancement experiments for which the nanoparticle pattern has been transferred to a non-photovoltaic substrate.

1. Introduction

Nowadays, it is well known that structures of metallic nanoparticles produce large plasmonic enhancements^[1,2] in a wide variety of optical processes such as fluorescence (FL) emission or Raman scattering. These enhancement effects have found a large number of applications in very active research and technological fields such as photonics, nano- or bio-technology. A variety of sophisticated lithographic and chemical techniques have been already developed to produce optimized metal structures. However, the complexity of the fabrication processes strongly limits the possibility of easily obtaining versatile plasmonic structures. Recently, a novel optoelectronic method to produce micrometric patterns of micro- and nanoparticles highly correlated with exciting light patterns has been developed. It is known as photovoltaic tweezers (PVT) and the details and fundamentals of the method have been summarized in some previous review papers.^[3-5] It is based on the dielectrophoretic and electrophoretic forces acting on neutral and charged particles, respectively, resulting from the evanescent photovoltaic (PV) electric fields generated by light illumination on a PV crystal such as $\text{LiNbO}_3\text{:Fe}$. The method was first applied to dielectric particles,^[6,7] but it works adequately regardless the electronic structure of the particles, which can be insulating, semiconducting or

metallic.^[4] The possibility of using this technique to generate particle patterns for applications such as charge sensors,^[8] diffractive optical devices^[9] or manipulation of bio-objects^[10] has been recently demonstrated. Patterns assembled from metallic nanoparticles should present new features associated to the localized surface plasmon resonances (LSPR) that have not been investigated so far. In particular, LSPR are known to strongly enhance the linear (absorption and luminescence) and nonlinear (second harmonic generation (SHG), Raman scattering) optical responses of a medium placed close to the nanoparticles.^[11,12] Currently, different alternative techniques, using optical methods, are employed to fabricate metallic nano-structures and to carry out plasmonic research. Among others, excimer laser irradiation of metal films has been reported to produce Ag-nanoislands arranged in self-organized patterns,^[13] which presents LSPR. Other relatively simple methods consist on precipitating Ag-nanoparticles in the frontiers of a periodically poled ferroelectric pattern under uniform UV light illumination^[14,15] or taking advantage of the pyroelectric effect.^[16-18] In this way, relevant enhancements in the SHG response have been obtained which are associated to the LSPR of the structures.^[19,20]

In comparison with other methods, our photo-assisted patterning procedure is inexpensive, flexible and reconfigurable, thus facilitating to test and compare the optical behaviour of different structures. In other words, the PVT technique can provide an attractive simple and versatile method to fabricate plasmonic platforms for optical enhancement applications. Although the method requires, in principle, a PV substrate, a novel achievement has been the possibility of transferring the generated patterns onto a non-PV substrate, such as glass or a polymer.^[9] This largely expands the potential of the method to include semiconducting and waveguiding devices.

This paper reports for the first time, the plasmonic effects presented in metallic patterns produced by PVT. To this end, we have prepared silver nanoparticle patterns since Ag

(together with Au nanoparticles), are the most widely used metals for the investigation of plasmonic phenomena and applications. Specifically, we have investigated the FL enhancement of different molecules placed in the close vicinity of the nano-scale structure of the PV metal patterns. The one-dimensional (1D) and two-dimensional (2D) structures used in our experiments have been fabricated from Ag nanoparticles, having 25 nm diameter, deposited on $\text{LiNbO}_3\text{:Fe}$ substrates. The increase of the scattering yields has been investigated by optical microscopy and reflectivity. As a first example of enhancement effects, we have deposited Disperse Red 1 (DR1) luminescent organic molecules on top of the PV nanoparticle patterns, in order to investigate the plasmonic effects of the structures on the red emission of the dye molecules. Optical microscopy, as well as micro-luminescence profiling, have been used to observe and quantify enhancement effects in the FL emission. For a biological application, PV patterns have been used to enhance the luminescence of chromophores (fluorescein) used as sensitizers for DNA and protein molecules. Finally, additional experiments have been performed with metallic patterns transferred from the PV $\text{LiNbO}_3\text{:Fe}$ substrate to poly (methyl methacrylate) (PMMA) films doped with perylene orange (PDI-O), observing again a marked FL enhancement. Overall, this work brings to light the potential and versatility of plasmonic structures fabricated by PVT.

2. Fabrication and characterization of the metallic nano-structures

2.1 Preparation of the nanoparticle patterns

In order to produce the nano-structured metallic patterns, the PVT technique includes two steps that can be either simultaneous or successive: i) illumination of the PV substrate ($\text{LiNbO}_3\text{:Fe}$) with the suitable light intensity pattern to generate the PV fields, and ii) deposition of the nanoparticles under these PV fields. The sequential procedure is easier to implement and it is the one used in this work. In order to have a high PV effect for particle

trapping^[4,21] highly iron doped (0.25 % mol) LiNbO₃ plates were used as PV substrates. Their thicknesses were 0.5 mm or 1 mm. Depending on the pattern type, different experimental configurations have been preferred as justified elsewhere.^[22] *i)* *x*-cut crystals and sinusoidal illumination for 1D fringe patterns, and *ii)* *z*-cut crystals and illumination from a spatial light modulator for 2D patterns. In previous work, it was demonstrated that this technique works well with nanoparticles having diameters d in the range of 40 – 100 nm.^[21,23,24] The present experiments use smaller Ag-nanoparticles, $d \sim 25$ nm, in order to possibly maximize plasmonic effects. They have been deposited from a hexane suspension in which the LiNbO₃:Fe substrate was immersed during 30 – 60 s. More details on the deposition method can be found elsewhere.^[4,24] When necessary, the metallic patterns generated on LiNbO₃ surface have been transferred to other substrate by a simple method^[9] using a thermal release tape (see Experimental Section for details).

2.2 Characterization of plasmonic patterns

1D and 2D periodic patterns have been fabricated by the PVT method described in Section 2.1. Good quality patterns over areas up to 1 cm² have been obtained. For the 1D patterns, different fringe spacings (from some tens to a few micrometers) and fringe widths were achieved. Optical microphotographs of two representative patterns are displayed in **Figure 1**. For the 1D pattern (Figure 1a), obtained on a *x*-cut sample, the spatial period Λ is 27 μm and the fringe width around 2 – 3 μm . Figure 1b shows a 2D pattern, prepared on a *z*-cut sample, consisting of a dense mosaic of squares with a side of $l = 200$ μm . Below those figures, a small region of each pattern is visualized through crossed polarizers and large magnification ($\times 1000$) to illustrate the details of their structure with a high contrast. This configuration strongly reduces the light background noise in the photographs.

Those figures reveal that the fringes and squares of the periodic patterns are not continuous, but show a discrete nanometer-scale structure including a variety of clusters of nanoparticles of different sizes. A SEM image of this nanostructure for a typical fringe of the 1D pattern is displayed in Figure 1c. The insets in figures 1a and 1b show a large diversity of colours, from red to blue, arising from the wavelength selectivity of the plasmonic scattering, due to the dependence of the LSPR on the cluster size and shape.^[25,26]

Optical reflectance from 400 to 1000 nm offers an additional and simple technique for an overall characterization of the patterns and their plasmonic effects. The overall reflectance of the 1D and 2D patterns are displayed in **Figure 2**, showing the ratio R/R_{LBN} , where R and R_{LBN} are, respectively, the reflectance of the patterned sample and that for the bare $\text{LiNbO}_3\text{:Fe}$ substrate taken as a reference. They show that the reflectance ratio of the samples decreases by about 5% for the 1D and by up to 20% for the 2D patterns in the wavelength range (300 – 500 nm). In the latter case, the ratio recovers to an intermediate value of 10% for $\lambda > 700$ nm. The experimental data on a large number of patterns confirm that the overall reflectance decreases on increasing coverage i.e. in accordance with the higher density of scatters, which contributes to the overall extinction of the sample. The spectral profiles illustrated in Figure 2a and 2b, do not show sharp bands, but only broad features that should correspond to the overlapping of the resonant plasmonic bands of the contributing nano-features present in the patterns and clearly apparent in Figure 1. Note that the plasmonic responses extend along a broad spectral range, thus facilitating the spectral tuning for enhancement effects.

3. Enhancement effects of plasmonic patterns

3.1 Plasmonic enhancement effects for the fluorescence of the DR1 dye

In order to study the enhancement effects produced by the PV nanoparticle patterns, we have investigated the fluorescence of dye molecules deposited on the samples. Specifically, we have first used DR1 molecules,^[27] that have found many applications in optical switching and optical data storage.^[28,29] The absorption and luminescence spectra associated to $\pi \rightarrow \pi^*$ transition are shown in **Figure 3**. The absorption band extends roughly from 400 nm to 550 nm and the luminescence emission, having a quantum efficiency of around 10^{-3} , is centered at about 570 nm. The chemical structure of this roughly linear molecule is shown as an inset in the figure.

The DR1 molecules are uniformly deposited on the surface of the previously patterned substrates by immersing them into an ethanol solution of the dye molecules. After evaporation of the solvent, the dye uniformly covers the sample surface. A first inspection of the luminescent pattern is shown in **Figure 4a**. It displays an optical microscope image (under white light illumination) for the 1D pattern of Figure 1a, after its coverage with the DR1 molecules. In order to enhance the contrast of the image, we have used again crossed polarizers between illumination and detection. An intense FL red emission is preferentially observed in close correlation with the pattern fringes. In fact, one sees brilliant red spots in correlation with the nanostructures constituting the fringes, where strong LSPR effects are expected. To reinforce this conclusion, the luminescent patterns have been investigated by FL microscopy excited at 530 nm. An image of the sample is shown in **Figure 4b**. Again, a strong red emission coming from the fringes can be observed, whereas the inter-fringe spacing looks essentially dark. Finally, for a more quantitative appraisal of the plasmonic enhancement effects on the dye fluorescence, the profile obtained by a micro-fluorescence scan of the pattern (excited at 488 nm) along a direction perpendicular to the fringes is displayed in **Figure 4c**. The scan profile shows a clear correlation with the periodic 1D pattern showing pronounced maxima with the same periodicity. From the figure, an average

FL enhancement factor around 10 has been obtained as the ratio between the maximum and the inter-fringe fluorescence values.

A similar experiment has been performed for the 2D square patterns after deposition of the DR1 dye. The corresponding FL microscope image and the scanned fluorescence profile along the direction perpendicular to a square side are, respectively, illustrated in **Figure 5a** and **5b**. A strong and sharp enhancement of the FL yield is observed when crossing the boundary of the squares. From Figure 5b, an average plasmonic FL enhancement factor of around 10 is measured, similar to that obtained for the 1D pattern.

This value is within the range of reported values for the enhancement factors of diverse plasmonic systems. Among others, enhancement factors of 5 and 50 have been achieved for Atto680 and indocyanine green (ICG) dyes, respectively, placed nearby Au metallic nano-systems whose LSPR overlaps with the dye emission band.^[30,31] A factor 8 was obtained in another system with Cy5 dye molecules, where the LSPR linked to arrays of Ag-nanoparticles matches both absorption and emission bands of the dye.^[32] Moreover, in a recent work concerning SHG,^[33] the authors use Ag-metallic structures (formed by aggregates) on RTP crystals, a structure rather similar to our PV patterns. The enhancement factor in our FL experiments (around 10) is somewhat higher than that obtained in the SHG experiments (factor 5) when the SH frequency matches the plasmon resonance of the nano-structure. On the other hand, the FL enhancement is lower than that achieved (factor 60) for the SH yield when the plasmon resonance nearly coincides with the fundamental excitation frequency. Note that in this later case, the SH yield varies with the square of the fundamental intensity and so, the meaningful value to be compared with the FL enhancement factor would be around $\sqrt{60} \sim 8$. In short, the FL enhancement factor in the present experiments is in most cases somewhat higher than other reported values probably because the plasmonic resonance of our metallic structures overlaps with both the emission and excitation dye band, enhancing

the two mechanisms. Hence, large Stokes shifts between absorption and emission dye bands have little relevance on the enhancement factor due to the broad plasmonic bands provided by PV structures.

3.2 Fluorescence enhancement experiments on biological molecules

A similar experiment to the one of the previous section has been carried out to demonstrate the applicability of the nanoparticle metallic structures in biotechnology. An Ag fringe pattern deposited on the PV substrate, similar to the one of Figure 1, was used in these experiments. Two solutions containing two distinct fluorescein-labeled molecules, with high biological interest, have been employed (see Experimental Section for details): *i*) DNA fragments with a maximum size in the range of 70–170 nm. *ii*) Synthetic peptide nucleic acid (PNA). The DNA probe is typically used in Fluorescent In Situ Hybridization (FISH) experiments, which serve to specifically localize DNA sequences (genes, etc.) in chromosomes, DNA fibers, tissues, and cells.^[34,35] The peptide is commonly used to detect human and other vertebrate telomeres by FISH, either with scientific and clinic interest.^[36] A 10 μ l droplet of each solution was deposited on two separated regions of the substrate surface. The sample was inspected by conventional optical and, subsequently, by FL microscopy and the resulting images are shown in **Figure 6**. It includes four images: Figure 6a and 6b present the corresponding optical microscope images, and Figure 6c and 6d the fluorescence images. Note that the optical and the fluorescence images show the same optical field, which corresponds to a region in the boundary of the DNA (Figure 6a and 6c) and the PNA solution droplets (Figure 6b and 6d), respectively.

One can clearly distinguish two regions in all photographs: on the left side, the area where the Ag pattern is covered by the droplet and, on the right side, the region with the nude pattern. It

is remarkable that as in the previous experiments (see Section 3.1) fluorescent light only comes from the points where the solution is close to the Ag-nanoparticles, being undetectable in the inter-fringe area. Hence, with the fluorescent microscope one can observe the pattern structures only inside the droplets. Thus, the results confirm again the plasmonic luminescence enhancement associated to the Ag-patterns and the applicability of the PV patterned samples in biological imaging and sensing. Note that, in this experiment, the enhanced fluorescent light is green instead of red, showing the broad wavelength range of plasmonic enhancement effects exhibited by the patterns, as expected from their broad reflectance spectra (see Figure 2).

3.3 Experiments on PMMA films containing perylene orange

So far, the enhancement experiments have involved nanoparticle patterns on top of a PV substrate due to the fabrication procedure. In this section, we remove this limitation by using a technique to transfer the metallic nanoparticle patterns to another non PV functional substrate.

The samples used here consisted on PMMA films containing 1 wt% of PDI-O deposited over glass, on top of which the Ag nanoparticles pattern originally fabricated on $\text{LiNbO}_3\text{:Fe}$, were transferred as described in Experimental section. PDI-O is a quite photo-stable molecule with a very high FL quantum yield (close to 1) when dispersed at concentrations of 1 wt%, or below, in inert thermoplastics polymers such as PMMA and polystyrene. These systems have shown a very good performance as active material in waveguide-based organic lasers.^[37,38]

Moreover, the potential of distributed feedback lasers based on this active system as refractive index^[39] or biological^[40] sensors has been recently demonstrated. The chemical structure of PDI-O and the absorption and FL spectrum of the film used in this work are shown in **Figure 7a**. In turn, **Figure 7b** shows an optical microscope image of the prepared plasmonic sample with the Ag-nanoparticle pattern on the luminescent PMMA film.

It can be clearly seen that the orange light, corresponding to the PDI-O fluorescence, mostly comes from the molecules lying just below the fringes of the deposited pattern of nanoparticles. Since the distribution of dye molecules is uniform, this result indicates that the dye FL yield is enhanced for those molecules that are in the vicinity of the nanoparticles. The effects appear less pronounced than those obtained in the previous experiments of section 3.1, probably because the density of particles is lower. Since the polymer film constitutes a light waveguide, the result is an illustrative example of the applicability of our plasmonic structures for integrated devices. Moreover, the good performance of PDI-O doped polymer films for laser applications, combined with this FL enhancement results open up a promising route^[19] for improving the laser efficiency.

5. Experimental Section

Materials: *x*-cut (1 mm thick) and *z*-cut (0.5 and 1 mm thick) wafers of LiNbO₃ doped with 0.25% mol of Fe were used as PV substrates. They were bought to Hangzhou Freqcontrol Electronic Technology Ltd., and cut obtaining samples with surface dimensions around 10 × 6 mm². Spherical Ag-nanoparticles with an average particle size (APS) of 25 nm and 99.95% purity were supplied by Skyspring Nanomaterials, Inc. In Figure 8, SEM image of the nanoparticles is provided. DR1 powder, with a dye content of 95% (bought to Sigma-Aldrich Co.) was dissolved in ethanol with a concentration of around 1 g/l. The DNA probe was obtained by nick translation with Fluorescein-12-dUTP of red kangaroo (*Macropus rufus*) genomic DNA, following the standard protocol indicated in the BIO-PROBE Nick Translation Kit. This method renders labeled DNA fragments (probes) with a maximum size in the range of 200–500 bp, where the fluorophore-12-dUTP has replaced the DNA deoxythymidine triphosphate (dTTP) positions. The peptide is a commercial Fluorescein IsoTioCyanate (FITC)-labeled (C₃TA₂)₃ PNA probe (Applied BiosystemsTM), premixed in hybridization

solution and ready to use and belongs to a wide family of commercial FISH probes with different specificities and purposes.^[41] The FL film was obtained depositing PMMA with 1 wt% of PDI-O, over glass by spin-coating.

Methods: The illumination of the LiNbO₃:Fe substrates, to induce the PV electric fields, has been carried out with a cw frequency-doubled Nd:YAG laser (Verdi model from Coherent) providing 5 W at $\lambda = 532$ nm. The typical light intensities on the sample are in the range of 1 – 100 mW/cm². 1D sinusoidal light patterns have been generated by two-beam interference (holographic configuration), while 2D periodical light patterns by image projection using a amplitude/phase spatial light modulator (Holoeye, LC-R1080 model). After illumination, substrates were immersed during 30–60 s in a hexane suspension of Ag nanoparticles, where particle deposition takes place. To assure a homogeneous deposition of the dye molecules, the PV field, responsible for the silver trapping, is thermally erased by sample heating (250°C during 10 minutes), before dye deposition. Optical microscope images have been taken with a Nikon Eclipse 80i microscope in reflection configuration. In order to enhance the contrast of the image, crossed polarizers between illumination and detection have been used for eliminating the background reflectance coming essentially from the LiNbO₃:Fe substrate. For FL microscopy characterization, a Leica DMLB FL microscope equipped with an external light source with metal halide bulb (Leica EL600) and three low-pass band filters for visualization of red, green and blue FL, has been employed. For the visualization of fluorescein-labeled specimens, a LED illumination system (pE-300white, from CoolLED Ltd.) has been used as light source. For micro-fluorescence measurements, the sample was placed in a confocal microscope provided with a motorized stage. A microscope objective (giving a spot diameter of 0.5 μ m) was used to focus the 488 nm laser excitation and collect the FL that, after passing several filters, was dispersed and analysed with a high sensitivity Si CCD camera (Synapse, Horiba) attached to a monochromator (iH320, Horiba). The

nanoparticle pattern has been transferred from the $\text{LiNbO}_3\text{:Fe}$ substrate to a PMMA+PDI-O film by using a thermal release tape (supplied by Graphene Supermarket, Graphene Laboratories Inc.) following a simple method described in reference [22]. The tape is stuck to the PV substrate surface and peeled off with the particles attached on it. Then, the tape is firmly stuck to the PMMA film and came off after a smooth heating process at 110 °C during a few minutes. The result reproduces the micrometric pattern in the new substrate with a fraction of transferred particles of around 40–50%.

6. Conclusion

The technique usually designated as PVT has been applied for the first time to fabricate plasmonic metallic nano-structures at the surface of a $\text{LiNbO}_3\text{:Fe}$ crystal. The structures are generated by light-induced patterning of Ag particles with 25 nm diameter. Periodic 1D and 2D structures, presenting a nanometer-scale structure with a variety of cluster sizes, have been achieved. The structures show plasmonic features that are revealed by a strongly wavelength selective light scattering. The LSPRs have allowed inducing significant FL enhancement effects on a variety of dye molecules (DR1, fluorescein and PDI-O), emitting along the whole visible range, that have been deposited on top of particle patterns previously prepared on $\text{LiNbO}_3\text{:Fe}$. Specifically, from micro-luminescence scanning experiments with DR1 dye, a strong FL enhancement factor of around 10 has been measured for the patterned 1D and 2D nanostructures. Finally, a FL enhancement connected with the plasmonic patterns has been also observed in two additional systems with high scientific and technological interest: fluorescein labelled biomolecules (DNA and peptides) and luminescent organic laser films.

The whole set of experiments stand out the potential of the PVT method to prepare plasmonic platforms, useful to induce enhancement of FL emission and very likely of other linear and nonlinear phenomena. The main advantage of the technique is the flexibility to change the

geometry of the patterned structures and also, to handle nanoparticles with different shapes and sizes on the PV substrate. Besides, the metallic structure can be transferred to any other convenient substrate. Moreover, the technique provides broad bands extending from blue to the infrared, which result from the overlapping of individual plasmonic resonances. This feature allows a flexible spectral tuning of the plasmonic resonance, as shown by the different organic dye wavelength ranges used in the experiments. From the obtained results, a large variety of applications are suggested or even demonstrated, such as plasmonic enhancement of luminescence for imaging and sensing in biotechnology or fabrication of functional materials and devices with improved properties (plasmonic integrated optical devices, plasmonic nano-lasers or solar cells, etc.).

Acknowledgements This work was supported by the funding of the Ministerio de Economía y Competitividad of Spain under the project MAT2014-57704-C3. M. A. Díaz also acknowledges Spanish Government (MINECO) and the European Community (FEDER) through Grant MAT2015-66586-R.

Received: ((will be filled in by the editorial staff))

Revised: ((will be filled in by the editorial staff))

Published online: ((will be filled in by the editorial staff))

References

- [1] W. L. Barnes, A. Dereux, T. W. Ebbesen, *Nature* **2003**, 424, 824.
- [2] D. A. Genov, A. K. Sarychev, V. M. Shalaev, A. Wei, *Nano Lett.* **2004**, 4, 153.
- [3] J. Villarroel, H. Burgos, A. García-Cabañes, M. Carrascosa, A. Blázquez-Castro, F. Agulló-López, *Opt. Express* **2011**, 19, 24320.
- [4] M. Carrascosa, A. García-Cabañes, M. Jubera, J. B. Ramiro, F. Agulló-López, *Appl. Phys. Rev.* **2015**, 2, 040605.

- [5] M. Esseling, *Photorefractive optoelectronic tweezers and their applications*, Springer thesis, Springer, Heidelberg, Germany **2015**.
- [6] S. S. Sarkisov, M. J. Curley, N. V. Kukhtarev, A. Fields, G. Adamovsky, C. C. Smith, E.L. Moore, *Appl. Phys. Lett.* **2001**, 79, 901.
- [7] H. A. Eggert, F. Y. Kuhnert, K. Buse, J. R. Adleman, D. Psaltis, *App. Phys. Lett.* **2007**, 90, 241909.
- [8] M. Esseling, A. Zaltron, C. Sada, C. Denz, *Appl. Phys. Lett.* **2013**, 103, 061115.
- [9] J. F. Muñoz-Martínez, M. Jubera, J. Matarrubia, A. García-Cabañes, F. Agulló-López, M. Carrascosa, *Opt. Lett.* **2016**, 41, 432.
- [10] M. Jubera, I. Elvira, A. García-Cabañes, J. L. Bella, M. Carrascosa, *Appl. Phys. Lett.* **2016**, 108, 023703.
- [11] F. Hao, P. Nordlander, M. T. Burnett, S. A. Maier, *Phys. Rev. B* **2007**, 76, 245417.
- [12] V. Giannini, A. I. Fernández-Domínguez, S. C. Heck, S. A. Maier, *Chem. Rev.* **2011**, 111, 3888.
- [13] J. Peláez, C. N. Afonso, J. Bulír, M. Novotný, J. Lancok, K. Piksová, *Nanotechnology* **2013**, 24, 095301.
- [14] X. Liu, K. Kitamura, K. Terabe, H. Hatano, N. Ohashi, *Appl. Phys. Lett.* **2007**, 91, 044101.
- [15] Y. Sun, R. J. Nemanich, *J. Appl. Phys.* **2011**, 109, 104302.
- [16] S. Grilli, P. Ferraro, *Appl. Phys. Lett.* **2008**, 92, 232902.
- [17] S. Grilli, S. Coppola, G. Nasti, V. Vespini, G. Gentile, V. Ambrogio, C. Carfagna, P. Ferraro, *RSC Adv.* **2014**, 4, 2851.

- [18] A. Gallego, A. García-Cabañes, M. Carrascosa, L. Arizmendi, *J. Phys. Chem. C* **2016**, *120*, 731.
- [19] E. Yraola, P. Molina, J. L. Plaza, M. O. Ramírez, L. E. Bausá, *Adv. Mater.* **2013**, *25*, 910.
- [20] L. Sánchez-García, M. O. Ramírez, P. Molina, F. Gallego-Gómez, L. Mateos, E. Yraola, J. J. Carvajal, M. Aguiló, F. Díaz, C. de las Heras, L. E. Bausá, *Adv. Mater.* **2014**, *26*, 6447.
- [21] H. Burgos, M. Jubera, J. Villarroel, A. García-Cabañes, F. Agulló-López, M. Carrascosa, *Opt. Mater.* **2013**, *35*, 1700.
- [22] J. F. Muñoz-Martínez, I. Elvira, M. Jubera, A. García-Cabañes, J. B. Ramiro, C. Arregui, M. Carrascosa, *Opt. Mater. Express* **2015**, *5*, 1137.
- [23] X. Zhang, J. Wang, B. Tang, X. Tan, R. A. Rupp, L. Pan, Y. Kong, Q. Sun, J. Xu, *Opt. Express* **2009**, *17*, 9981.
- [24] J. Matarrubia, A. García-Cabañes, J. L. Plaza, F. Agulló-López, M. Carrascosa, *J. Phys. D: Appl. Phys.* **2014**, *47*, 265101.
- [25] K. L. Kelly, E. Coronado, L. L. Zhao, G. C. Schatz, *J. Phys. Chem. B* **2003**, *107*, 668.
- [26] R. Esteban, R. W. Taylor, J. J. Baumberg, J. Aizpurua, *Langmuir* **2012**, *28*, 8881.
- [27] C. Toro, A. Thibert, L. De Boni, A. E. Masunov, F. E. Hernández, *J. Phys. Chem. B* **2008**, *112*, 929.
- [28] A. Natansohn, P. Rochon, *Chem. Rev.* **2002**, *102*, 4139.
- [29] Z. F. Liu, K. Hashimoto, A. Fujishima, *Nature*, **1990**, *347*, 658.
- [30] F. Tam, G. P. Goodrich, B. R. Johnson, N. J. Halas, *Nano Lett.* **2007**, *7*, 496.

- [31] O. L. Muskens, V. Giannini, J. A. Sánchez-Gil, J. Gómez-Rivas, *Nano Lett.* **2007**, *7*, 2871.
- [32] O. Stranik, H.M. McEvoy, C. McDonagh, B.D. MacCraith, *Sens. Actuators B* **2005**, *107*, 148.
- [33] L. Sánchez-García, C. Tserkezis, M. O. Ramírez, P. Molina, J. J. Carvajal, M. Aguiló, F. Díaz, J. Aizpurua, L. E. Bausá, *Opt. Express* **2016**, *24*, 8491.
- [34] M. Pita, J. Orellana, P. Martínez-Rodríguez, A. Martínez-Ramírez, B. Fernández-Calvin, J. L. Bella, in *Functional analysis of DNA and chromatin. Methods in Molecular Biology* (Ed. J. M. Walker, Humana Press), Springer Science+Business Media NY, USA **2014**. Ch. *FISH methods in cytogenetic studies*.
- [35] C. Cui, W. Shu, P. Li, *Front. Cell Dev. Biol.* **2016**, *4*, 89.
- [36] A. Viera, M. I. Ortiz, E. Pinna-Senn, G. Dalmasso, J. L. Bella, J. A. Lisanti, *Cytogenet. Genome Res.* **2004**, *107*, 99.
- [37] M. G. Ramírez, M. Morales-Vidal, V. Navarro-Fuster, P. G. Boj, J. A. Quintana, J. M. Villalvilla, A. Retolaza, S. Merino, M. A. Díaz-García, *J. Mater. Chem. C* **2013**, *1*, 1182.
- [38] A. Retolaza, A. Juarros, D. Otaduy, S. Merino, V. Navarro-Fuster, M. G. Ramírez, P. G. Boj, J. A. Quintana, J. M. Villalvilla, M. A. Díaz-García, *Microelectron. Eng.* **2014**, *114*, 52.
- [39] M. Morales-Vidal, P. G. Boj, J. A. Quintana, J. M. Villalvilla, A. Retolaza, S. Merino, M. A. Díaz-García, *Sens. Actuators B: Chem.* **2015**, *220*, 1368.
- [40] A. Retolaza, J. Martínez-Perdiguero, S. Merino, M. Morales-Vidal, P. G. Boj, J. A. Quintana, J. M. Villalvilla, M. A. Díaz-García, *Sens. Actuators B: Chem.* **2016**, *223*, 261.

[41] H. Shi, F. Yang, W. Li, W. Zhao, K. Nie, B. Dong, Z. Liu, *Biosens. Bioelectron.* **2015**, *66*, 481.

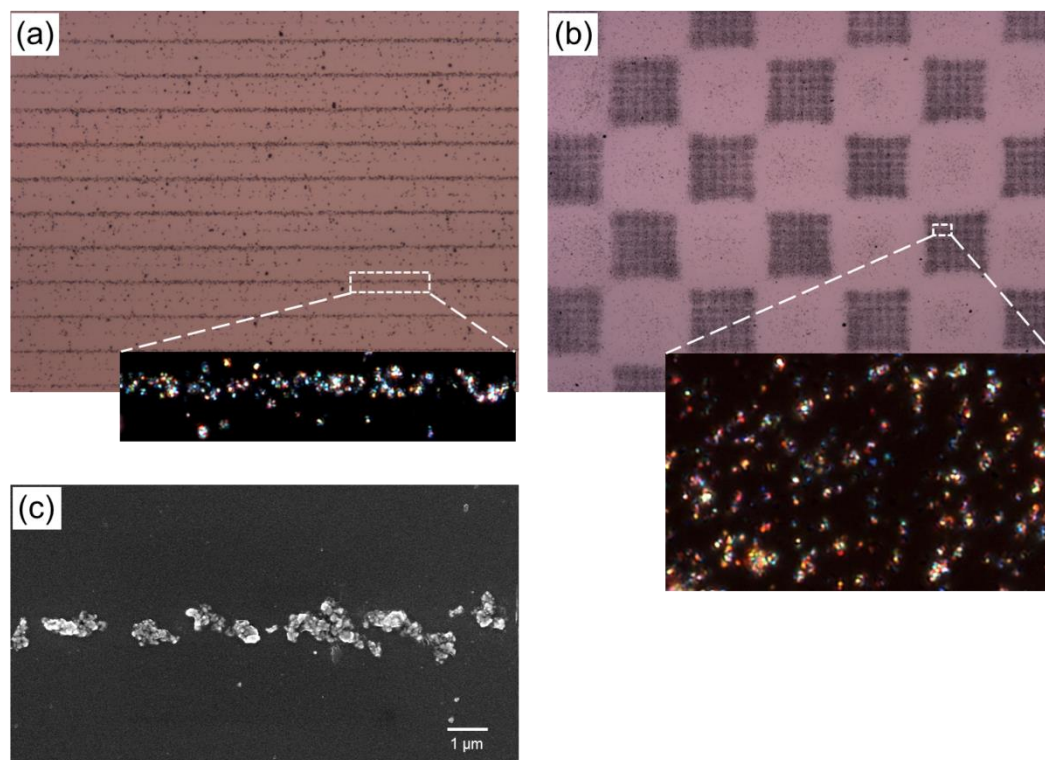


Figure 1. Microscopic images of periodic patterns of Ag-nanoparticles under illumination by (a) a sinusoidal light pattern with a spatial period $\lambda = 27 \mu\text{m}$ on an x -cut substrate, and (b) a mosaic of squares with side $l = 200 \mu\text{m}$ on a z -cut substrate. The corresponding insets show small regions of the patterns with higher magnification ($\times 1000$). (c) SEM image of a fragment of a typical fringe of the 1D pattern.

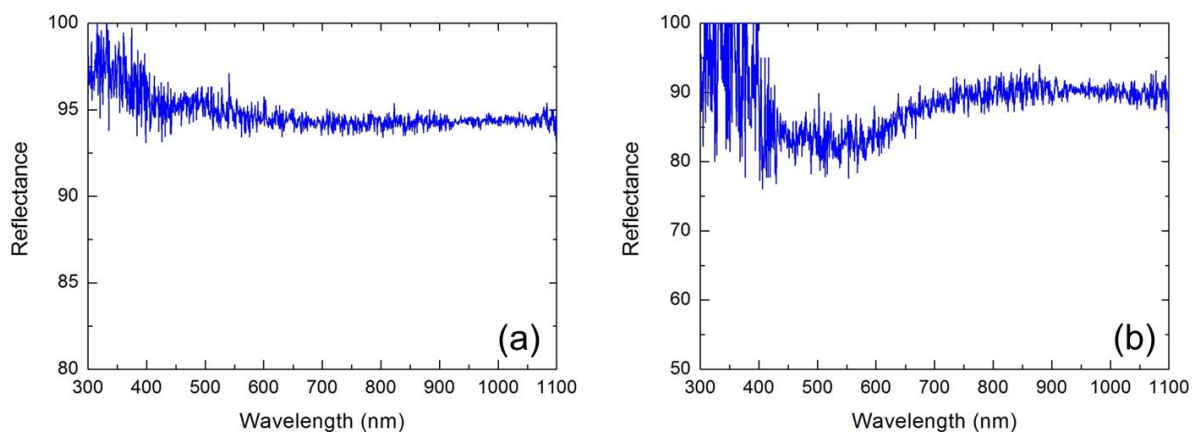


Figure 2. Spectra for the relative reflectance (sample reflectance normalized to the reflectance of the bare $\text{LiNbO}_3\text{:Fe}$ substrate as explained in the text) of the Ag-nanoparticle (25 nm diameter) patterns (a) Periodic lines ($\Lambda = 27 \mu\text{m}$), and (b) Square mosaic ($l = 200 \mu\text{m}$).

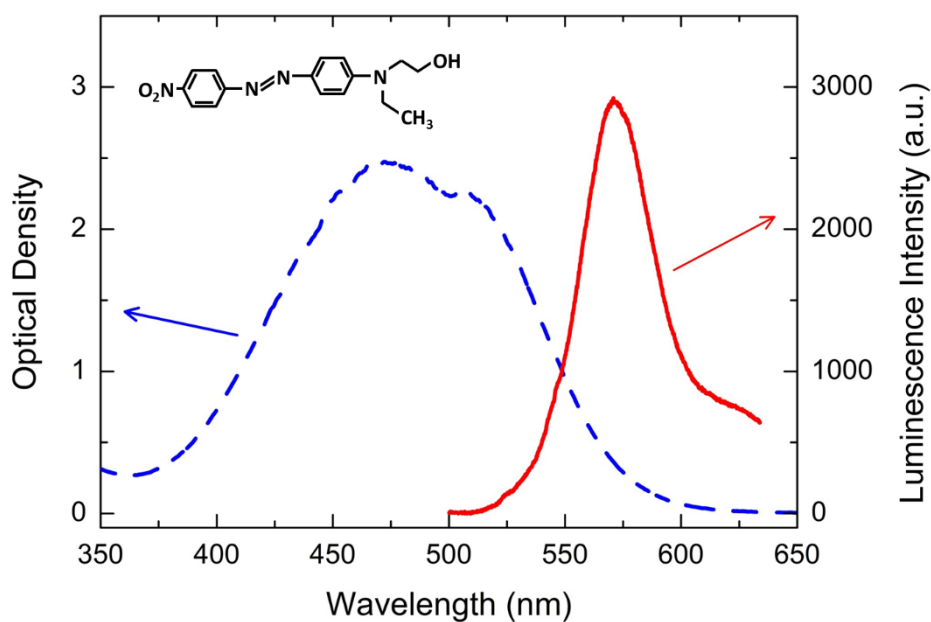


Figure 3. Absorption and FL spectra of DR1 dye in ethanol (95 % dye content). The inset shows the structure of the molecule.

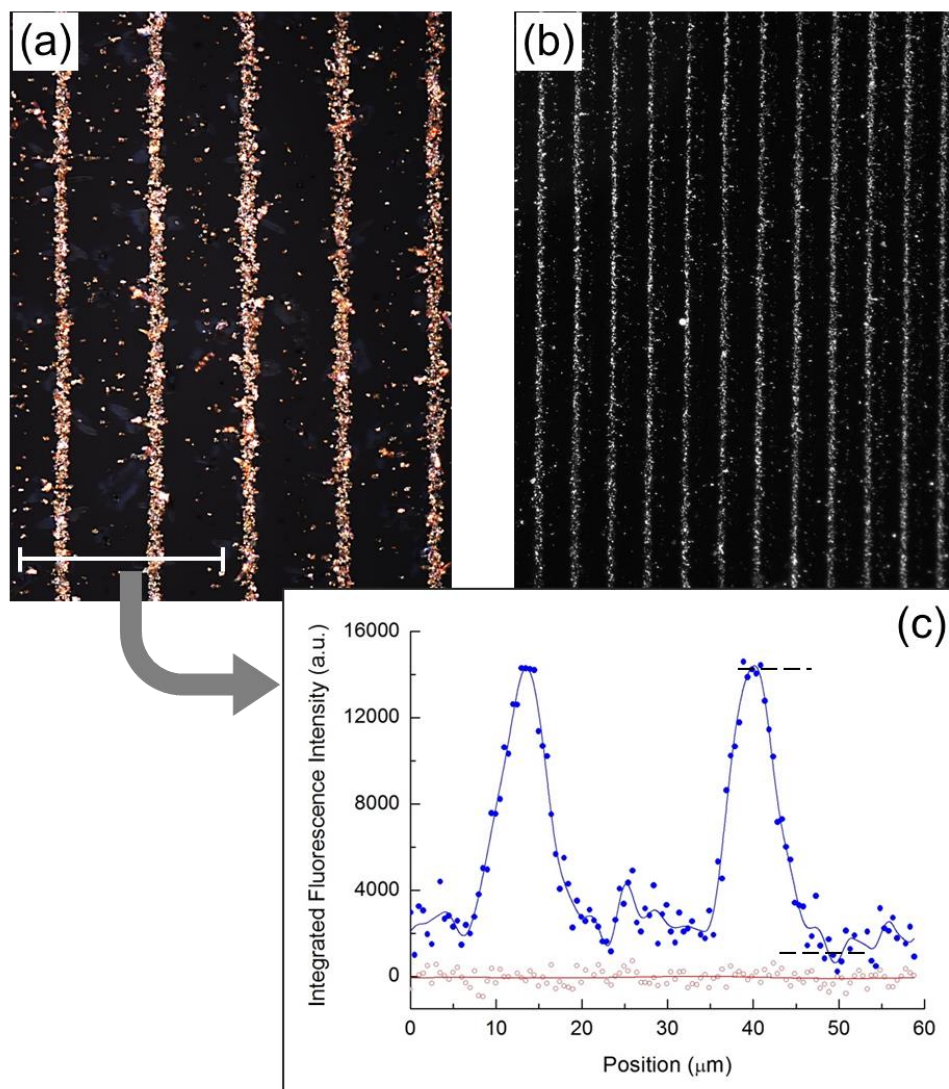


Figure 4. Micro-photographs of a periodic fringe pattern of Ag-nanoparticles covered with a DR1 dye film taken with (a) a conventional optical microscope or (b) a FL microscope (with black and white coupled camera). (c) Blue line: Overall FL intensity as a function of the position along a line perpendicular to the fringes as indicated in (a). Two dashed lines are drawn to mark the maximum and averaged intra-fringe levels. The red line indicates the zero FL intensity level measured in a region without dye.

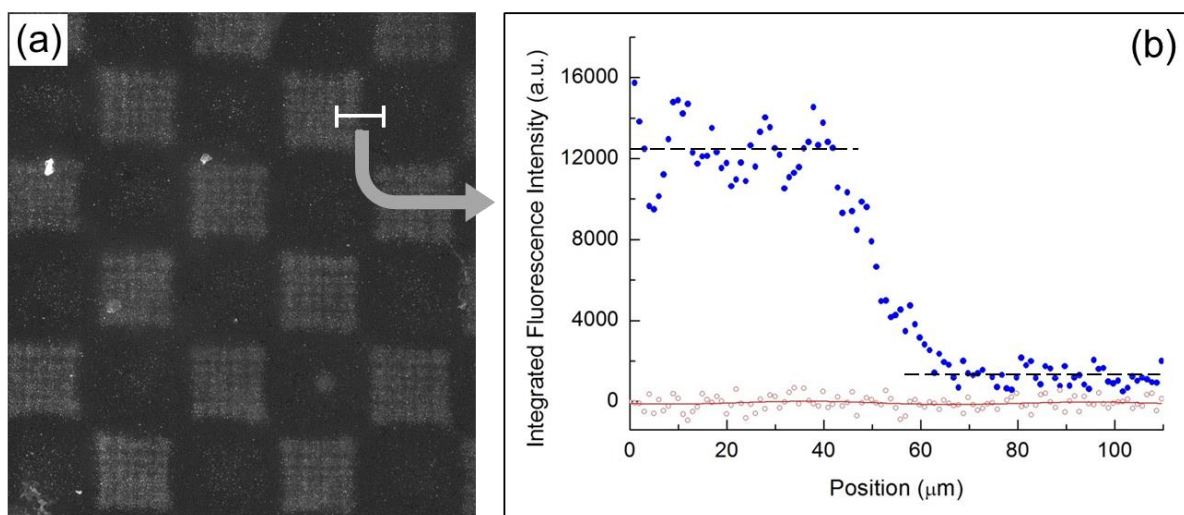


Figure 5. (a) Micro-photograph of a square pattern of Ag-nanoparticles covered with a DR1 dye film, taken with a FL microscope (with black and white coupled camera). (b) Overall FL intensity as a function of the position along a line perpendicular to a square edge as indicated in (a). The dashed lines are indicating the average FL levels in each region and the red line the zero level determined in a region without dye.

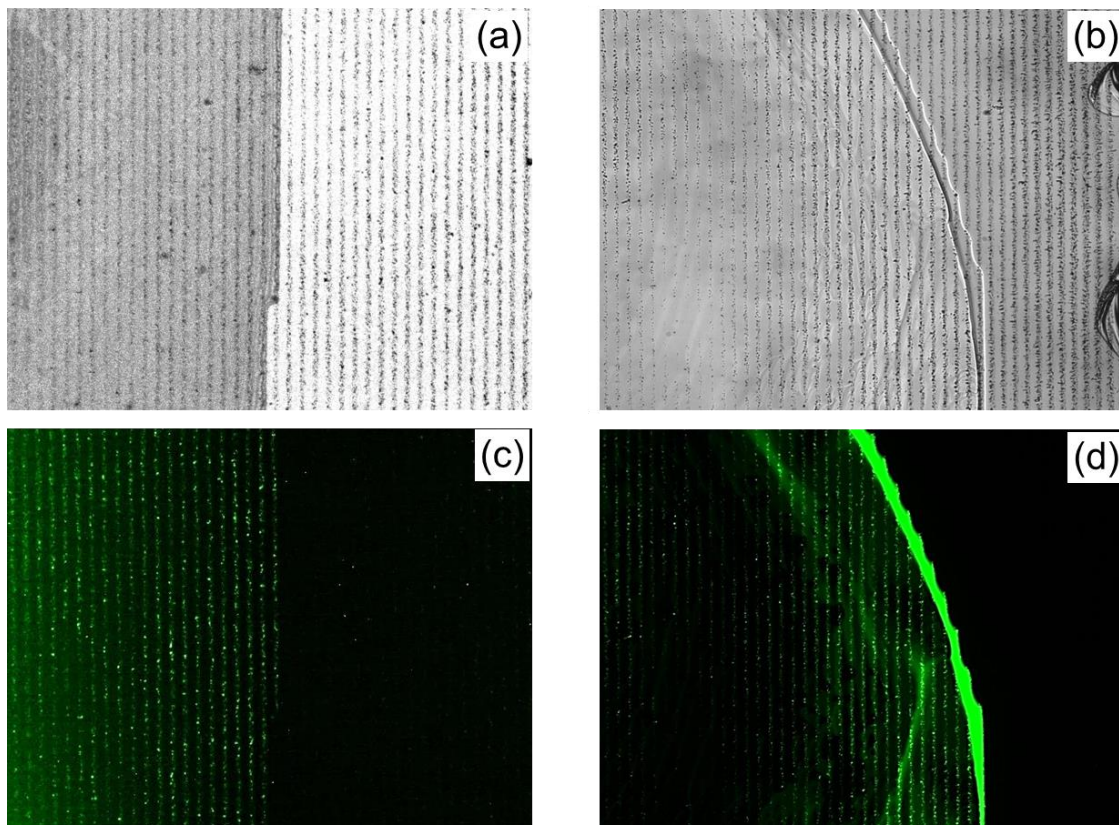


Figure 6. Optical microscope images (a) and (b), and FL microscope images (c) and (d), showing two droplets of fluorescein labelled biomolecules deposited on an Ag-nanoparticle periodic pattern: DNA for (a) and (c) and synthetic peptide for (b) and (d) solution droplets.

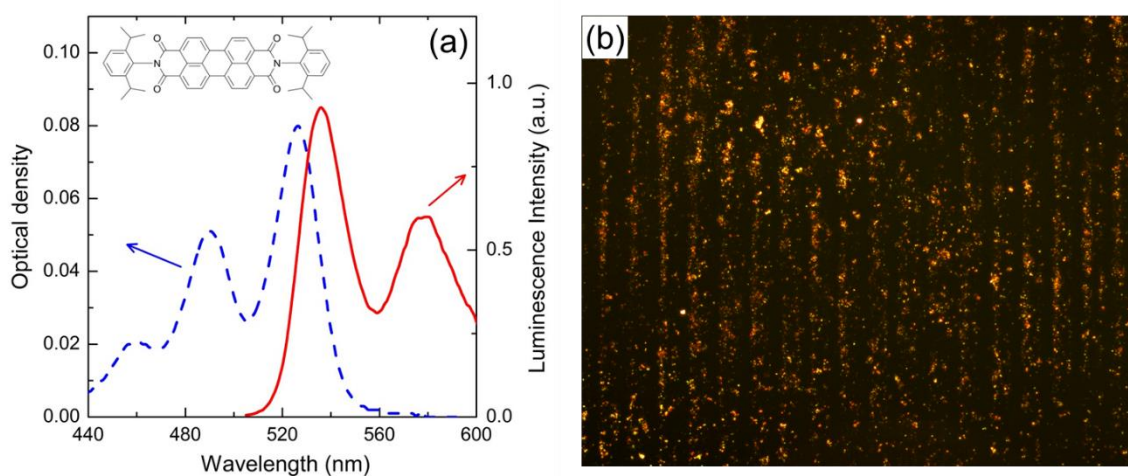


Figure 7. (a) Absorption and FL spectrum of a PMMA film containing 1 wt% of PDI-O. The inset shows the PDI-O chemical structure. (b) Microscopic image of the sample with a periodic 1D pattern of Ag-nanoparticles deposited on top of the surface, under white light illumination.

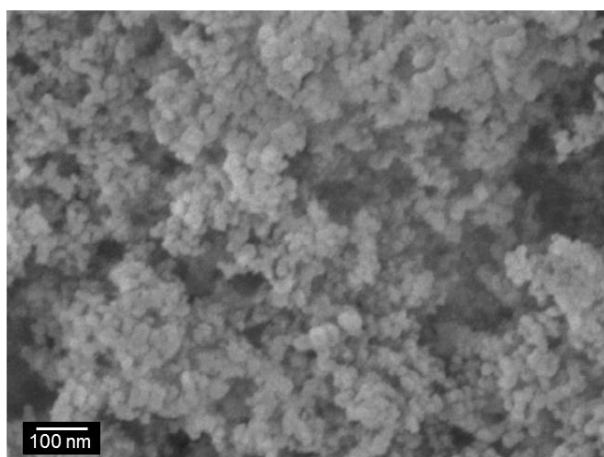


Figure 8. SEM image of the Ag nanoparticles (average particle size of 25 nm) used for PV trapping.